# Flow structures in a swirl flow - vortex breakdown condition

IOP Conf. Series: Journal of Physics: Conf. Series **1045** (2018) 012031 doi:10.1088/1742-6596/1045/1/012031

# Flow structures in a swirl flow - vortex breakdown condition

**P Novotny[1, 2], B Weigand[2], F Marsik[1], C Biegger[2] and M Tomas[1]**

[1] New Technologies - Research Centre, University of West Bohemia, Univerzitni 8, 30614 Plzen, Czech Republic
[2] Institute of Aerospace Thermodynamics, University of Stuttgart, Pfaffenwaldring 31, 70569 Stuttgart, Germany

E-mail: novotnyp@ntc.zcu.cz

**Abstract.** This paper presents an experimental and numerical analysis of swirl flow in a circular tube. Swirl flow is important for technical and natural processes, where high heat transfer and good fluid mixing are needed. Flow and vortex structures respecting redistribution of momentum and possible occurrence of vortex breakdown are taken into account. The swirl flow is analysed experimentally by the measurement of the velocity field using Particle Image Velocimetry (PIV) and numerically via the commercial CFD code ANSYS CFX. Three cases are investigated: laminar flow regime ($Re$ = 1,000), intermediate flow regime ($Re$ = 2,000), and turbulent flow regime ($Re$ = 5,000). The redistribution of the velocity field and the decrease of the swirl strength towards the outlet are shown. This redistribution affects the Reynolds number. Concerning the Rossby number, the occurrence of vortex breakdown in the swirl flow is determined. It is shown that the vortex breakdown takes place in the flow with higher Reynolds numbers, where an axial backflow may occur. Changes of the Reynolds numbers $Re_\phi$ and $Re_z$ along the tube length also confirm this statement. Furthermore, a thermodynamic perspective of vortex breakdown phenomena is presented.

## 1. Introduction

Swirl flow has an impact in several technical applications due to its influence on fluid mixing and heat transfer. Historically, swirl flow in a tube was investigated by Ranque in 1933 who discovered a temperature separation induced in this kind of flow [1]. Then, Hilsch [2] followed his work and studied the effects of geometry and operational parameters of the tube proposed by Ranque. Hence, this type of tube is nowadays known as Ranque - Hilsch vortex tube. Their general work was followed by many researchers and the problem of a swirl flow in a tube was investigated from different views.

Many authors were interested in a flow in an annulus with through flow and a rotating wall and its effect on heat transfer, e.g. the works [3-5]. They focused on the influence of co - and counter - rotating tubes on heat transfer in the case of heated outer tube. They found out the positive influence of an inner rotating tube on the heat transfer. Reich et al. [6] studied also the effect of rotation on laminar flow in a heated pipe resulting in the statement that free vortices occurring due to the heated pipe wall disappeared with increasing pipe rotation. Weigand and Beer [7] analysed the heat transfer in rotating tubes with respect to the flow pattern inside the tube. They observed a laminarisation of the flow due to tube rotation, which caused a decrease of the heat transfer. They extended the work to a case where a fluid entered a rotating tube in turbulent regime, i.e. the axial flow in the pipe was initially turbulent, a flow relaminarisation appeared by increasing rotation rate of the tube [8].

Hartnett and Eckert [9] analysed the effect of a rotating flow on an axial flow and heat transfer. They focused on measurements of the flow fields and the temperature in a vortex flow generated at nozzle cross - section area and moved in one direction to the end of the tube. Ligrani et al. [10] investigated flow phenomena in swirl chambers, which models a cooling passage located at the leading edge of a turbine blade, with significant axial and tangential velocity components. They carried out flow visualisations for different Reynolds numbers. They stated that the swirl flow could be very useful in different engineering applications, including biomedical applications, heat exchangers and automobile engines. Glezer et al. [11] focused on the internal swirling flow and its influence on the heat transfer. They used a test rig simulating a rotating leading edge internal passage of a blade with heated walls and a screw - shaped cooling swirl resulted from flow generated by tangential slots. They stated that Coriolis forces appearing during blades rotation had a positive influence on the internal heat transfer in case of the same direction of the Coriolis forces with the tangential velocity component. In contrary, there was observed the opposite phenomenon in case of the direction of the Coriolis forces acting in opposite direction of the swirl flow (tangential velocity).

The abrupt change in the flow structure resulting in a backflow is, in literature, referred as vortex breakdown [12]. This phenomenon might be observed due to flow over a delta wing influencing the lift and stability of the wing, and in an axisymmetric swirling flow in tubes. Vortex breakdown is usually characterised by a deformation and deceleration of the vortex core, changes of velocity distribution (with flow reversal), and changes of pressure distribution in the swirling flow. Thus, the occurrence of vortex breakdown has a strong influence on the performance of the studied system, such as turbines, trailing vortices behind a wing, cyclone separators, vortex tubes, swirl chambers, etc. The phenomenon of vortex breakdown was studied by researchers for decades and, as mentioned by Lucca - Negro and O'Doherty [13], there might be an association of flow instability to vortex breakdown. Moreover, some theories describing and explaining vortex breakdown were developed. Thus, there are three basic theories that are associated with vortex breakdown as stated by Escudier [14] or by Hall [15]

- instability, i.e. axisymmetric disturbances, spiral disturbances, non - linear interactions,
- stagnation, i.e. separation analogy, failure of slender core (quasi - cylindrical approximation),
- wave phenomena, i.e. inertia waves, solitary waves, shock or hydraulic jump analogy.

A criterion that may be used to predict the onset of vortex breakdown was proposed by Spall et al. [16]. This criterion was derived based upon previous experimental, numerical, and theoretical studies and followed work by Squire [17] and Benjamin [18]. The criterion is based on the Rossby number defined as the ratio of the axial velocity to the tangential velocity. A threshold for the occurrence of vortex breakdown, below which it might appear was, by Spall et al. [16], determined as 0.65. Furthermore, Spall et al. also concluded that this criterion is due to characteristic scales applicable to confined and unconfined vertical flows.

This contribution follows the above mentioned principles. Firstly, the experimental and numerical works are shortly introduced. Then, methodology used for flow field analysis is described. Thus, the Rossby number is used to predict vortex breakdown. To predict vortex breakdown, changes of tangential Reynolds number ($Re_\phi$) and axial Reynolds number ($Re_z$) towards tube outlet are used. Moreover, the decay of the swirl number, i.e. the decrease of the swirl strength of the flow, reflecting the redistribution of the flow inside the tube is represented also by the tangential Reynolds number ($Re_\phi$). Thermodynamic perspective of the vortex breakdown is discussed respecting the dissipation and destabilising processes during flow redistribution. The paper is closed by a summary and a conclusion.

## 2. Procedures

### *2.1. Experimental setup*

Flow measurements are conducted on a model swirl tube schematically depicted in Figure 1. A vacuum pump sucks air through the swirl tube and drives the open loop device. A laminar flow element is used to measure the mass flow rate into the swirl tube. Before the air approaches the swirl

generator, the air is seeded with oil particles for the PIV measurements. Then, the air flows through the swirl generator consisted of two tangential inlet slots (nozzles) into the swirl tube. The end of the tube represents the tube outlet connected via an outlet plenum guiding the flow to the vacuum pump.

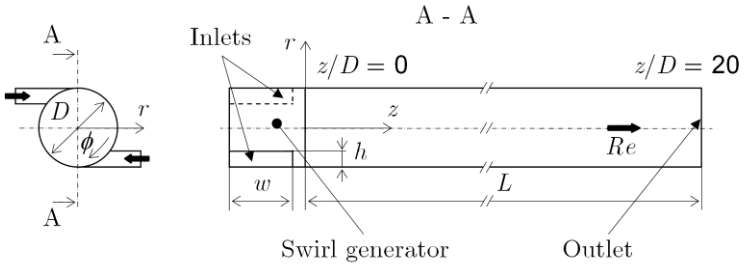


**Figure 1.** Swirl tube geometry including coordinate system.

The dimension of the swirl tube (Figure 1) are as follows: The inner diameter of the tube is $D$ = 50 mm, length of the tube is $L = 20D$. The swirl generator consists of two inlets with the height of $h/D$ = 0.1 and the width of $w/D$ = 0.67. This geometry results in a geometrical swirl number $S_{IG}$ = 5.3 given by equation (1).

$$S_{IG} = \frac{\pi R^2 (R - h/2)}{Rnwh}, \tag{1}$$

where $n$ denotes the number of tangential slots. The investigated Reynolds numbers range from 1,000 to 5,000 and the definition of the Reynolds number is given as

$$Re = \frac{\overline{U^z} D}{\nu} = \frac{4\dot{m}}{\pi D \mu}. \tag{2}$$

Here, $\overline{U^z}$ represents the exit bulk velocity, $D$ is the tube diameter, $\nu$ denotes the kinematic viscosity, $\dot{m}$ is the mass flow and $\mu$ is the dynamic viscosity. Table 1 summarises the range of investigated Reynolds numbers, corresponding bulk velocities and angular velocity taken from the experimentally obtained tangential velocity profile near the tangential inlets ($z/D$ = 0), where the tangential velocity profile corresponds to a solid body vortex. The axial bulk velocity and angular velocity will be used as parameters to plot results in dimensionless form. The axial velocity profile is measured in the tube axis over the whole length. Furthermore, the tangential velocity profile is measured at the positions $z/D$ = 0 - 19, which are one tube diameter ($D$) apart from each other.

**Table 1.** Investigated Reynolds numbers and corresponding axial bulk velocity, mass flow rate, angular velocity of solid body rotation and inlet velocities for numerical model.

| $Re$ (-) | $\overline{U^z}$ (m s$^{-1}$) | $\dot{m}$ (kg s$^{-1}$) | $\Omega$ (s$^{-1}$) | $U_{inlet}$ (m s$^{-1}$) |
|---|---|---|---|---|
| 1,000 | 0.3 | 0.0007 | 100 | 1.74 |
| 2,000 | 0.6 | 0.0014 | 200 | 3.48 |
| 5,000 | 1.5 | 0.0035 | 500 | 8.69 |

*2.2. Numerical model*

The numerical simulations are carried out for an isothermal turbulent flow with the commercial code ANSYS CFX, for modelling turbulence the BSLEARSM (Baseline Explicit Algebraic Reynolds Stress Model) model is employed [19]. In case of the lowest Reynolds number $Re$ = 1,000, the Gamma model is used to model transition to turbulence with default values of the onset Reynolds number $Re$ = 260 and the low turbulent intensity and eddy viscosity ratio. Usage of the Gamma model in case of the Reynolds number $Re$ = 2,000 was also tested, but no positive effect was observed. So that, in this case the Gamma model is not utilised. Thus, in the cases of the Reynolds numbers $Re$ = 2,000 and

*Re* = 5,000 only the medium turbulent intensity and eddy viscosity ratio and the high turbulent intensity and eddy viscosity ratio are set, respectively.

The domain for the numerical simulations is designed to be close as possible to the swirl tube depicted in figure 1. The tube diameter and dimensionless length are $D$ = 50 mm and $L/D$ = 20. The swirl generator consists of two inlets with the height of $h/D$ = 0.1 and the width of $w/D$ = 0.67. To correctly model the swirl generator, the total width of the swirl generator is large by the parameter 0.8$D$. So, that the total length of the domain is 21.47$D$.

The wall boundary conditions are set as no - slip conditions. Other details of these simulations respecting the different Reynolds numbers are listed in table 1. The swirl tube geometry is for the three Reynolds numbers meshed via hexahedral O - grids with a total mesh size of 1.1 million cells. The wall mesh is chosen to provide a dimensionless wall distance of $y_1^+ \leq 1$ for the first grid point near the wall. The time step is adjusted to comply the limit given by the Courant - Friedrichs - Lewy number (CFL) ≤ 1, which may ensure stability of the solution. In ANSYS CFX, the chosen time discretisation is expresses by a second order backward Euler scheme, and convective and viscous fluxes are approximated with high accuracy enabling the software usage of the second order upwind differencing scheme with a blending function to the first order upwind differencing scheme for better convergence. The numerical simulations are run for $3\Delta t_{domain}$ to ensure that the whole domain has been calculated and that simulations have already converged. Here, the time domain is $\Delta t_{domain} = L / \overline{U^z}$ .

### *2.3. Flow analysis*

#### *2.3.1. Velocity approximation*

The velocity field given by measurements and numerical simulations are analysed with respect to vortex breakdown, the swirl decay, and thermodynamic stability condition. According to these analyses smooth functions continuously distributed along the radial coordinate are desired. Thus, the obtained flow field is approximated (fitted) to get smooth curves. A model that is able to be used for the swirl flow in the tube is developed for an axisymmetrical helical vortex [20], which is, for our purposes, extended to capture the wall region of the swirl tube.

$$u^{\phi} = \frac{\Gamma}{2\pi r}\left[1-\exp\left(-\frac{r^2}{\varepsilon^2}\right)\right]\left\{1-\frac{1}{\exp\left[k\left(R-r\right)\right]}\right\}, \tag{3}$$

$$u^{z} = u^{0} - \frac{\Gamma}{2\pi l}\left[1-\exp\left(-\frac{r^2}{\varepsilon^2}\right)\right]\left\{1-\frac{1}{\exp\left[k\left(R-r\right)\right]}\right\}, \tag{4}$$

In these approximations, $\Gamma$ denotes the circulation, $\varepsilon$ is the vortex core size, $l$ is the pitch of helical symmetry, $u^0$ is the velocity at the vortex axis and $k$ is the wall parameter. These parameters are obtained via the free Toolbox EzyFit in Matlab [21].

#### *2.3.2. Rossby number*

Spall et al. [16] proposed a criterion based on the Rossby number that is used to predict the onset of vortex breakdown. Local values of the Rossby number are computed by the ratio of the axial velocity to the tangential velocity

$$Ro = \frac{u^{z^*}}{r^*\Omega}. \tag{5}$$

Here, $r^*$ defines the radial position where the swirl velocity reaches its maximum, $r^*\Omega$ is the swirl velocity where $\Omega$ denotes the angular velocity of the solid body rotation, and $u^{z*}$ is the axial velocity at the position $r^*$.

*2.3.3. Axial and tangential Reynolds number*

The axial Reynolds number and the tangential Reynolds number, equation (6), take into account mean values of the axial velocity and mean values of the tangential velocity measured and/or computed at the defined axial position of the tube.

$$Re_z = \frac{\overline{u^z} D}{\nu},\ Re_\phi = \frac{\overline{u^\phi} D}{\nu} \tag{6}$$

where $\overline{u^z}$ and $\overline{u^\phi}$ are the mean value of the experimentally and/or numerically obtained axial velocity and tangential velocity, $D$ represents the tube diameter and $\nu$ is the kinematic viscosity.

*2.3.4. Thermodynamic stability condition*

The stability concept based on thermodynamics follows the work by Marsik [22]. The thermodynamic stability condition (TSC function) can be, in general, written as

$$\bar{\pi} = T\sigma(S) \geq 0\,, \tag{7}$$

where $T$ is the thermodynamic temperature and $\sigma$ ($S$) represents a term covering the production of entropy. Equation (7) is valid for each point $x$ in the body with the volume $V$. Taking into account the balance of the total specific enthalpy $h_t$, the TSC function for cases without heat transfer can be rearranged to read

$$\pi = t_{dis}^{ik} \frac{\partial u_i}{\partial x^k} + u_i \frac{\partial t_{dis}^{ik}}{\partial x^k} \geq 0\,, \tag{8}$$

where $t_{dis}^{ik}$ is the Cauchy stress tensor for an incompressible fluid. The preliminary outcomes of this thermodynamic concept can be found in the work by Marsik et al. [23]. The flow is from a thermodynamic point of view stable if equation (8) is satisfied. A global value of the TSC function is computed by volume integration of equation (8).

However, to obtain values of the global TSC function in dimensionless form, the volume integral is normalised by the inner volume of the tube $V_t$, the material parameter $\mu$ (dynamic viscosity), and the angular velocity $\Omega$ taken from table 1.

$$\frac{\Pi}{V_t \Omega^2 \mu} = \frac{1}{V_t} \int_V \frac{\pi}{\Omega^2 \mu} \mathrm{d}\bar{V} \geq 0,\ \text{for}\ \mathrm{d}\bar{V} = \bar{r}\,\mathrm{d}\bar{\phi}\,\mathrm{d}\bar{r}\mathrm{d}\bar{z}\,. \tag{9}$$

The axial coordinate ($\mathrm{d}\bar{z}$) in the integral varies from zero to 1 mm and represents the thickness of the slice with a radius $r$ changing from 0 to $R$, for which a value of the global TSC function at a position $z/D$ is calculated. Moreover, there is a huge dissipation near the tube wall resulting in positive values of the global TSC function. On the other hand, due to the velocity redistribution in the tube, there are processes in the flow that the global TSC function should cover. Due to this hypothesis, the values of the global TSC function computed at a position ($z/D$) without the influence of the wall are used for the analysis of the flow field to present their development towards tube outlet. These values are computed by equation (9), where integration over the radial coordinate is taken from 0 to 0.9$R$.

## 3. Results

Data obtained from numerical results are extended by the profile near the tangential inlets (position $z/D$ = -1) where measurements are not possible. These data are shown in order to better comprehend the redistribution of the velocity field from the tube inlets to tube outlet.

Vortex breakdown can be predicted by a change of the two different Reynolds numbers, the axial Reynolds number ($Re_z$) and the tangential Reynolds number ($Re_\phi$), equation (6), respectively. In contrast to the analysis based on the Rossby number (equation 5), these Reynolds numbers are used to study the effect of the mean velocities. The decreasing trend of the calculated tangential Reynolds

numbers, given mainly by a drop of the swirl number characterising the swirl strength, and an almost constant trend of the axial Reynolds numbers at different positions are obvious from Figure 2. The axial and tangential Reynolds numbers are determined for all investigated Reynolds numbers.

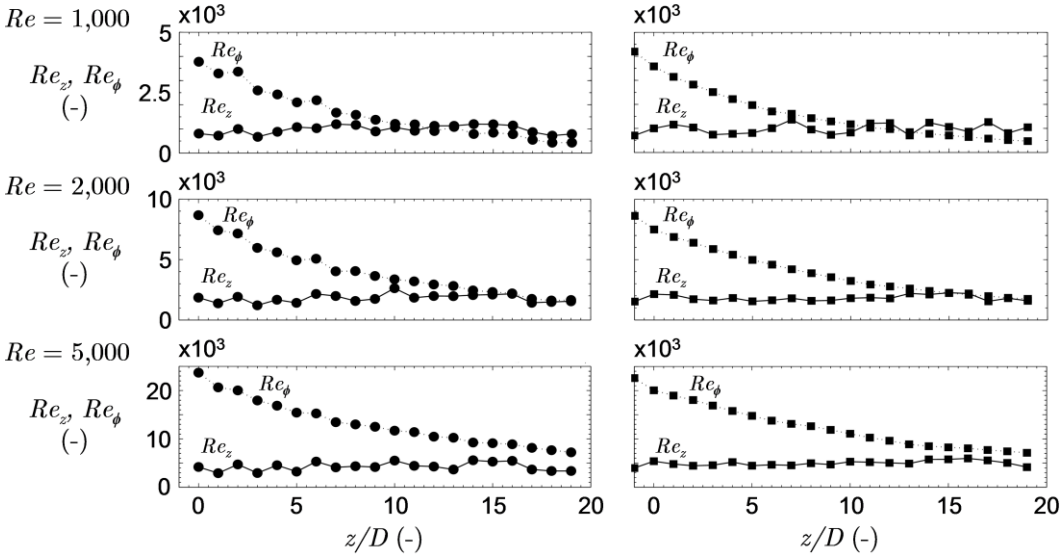


**Figure 2.** Evolution of the axial ($Re_z$) and tangential ($Re_\phi$) Reynolds number towards tube outlet. Bullets and squares represent experiment and numerics, respectively.

In case of *Re* = 1,000, the tangential Reynolds number is larger than the axial Reynolds number in the region near the tangential inlets. This indicates that in this region, vortex breakdown may occur. As the fluid approaches the tube outlet, the flow becomes axial dominant without axial backflow indicating no vortex breakdown. This fact is represented by intersection of the tangential and the axial Reynolds number followed by a drop of the tangential Reynolds number under the axial Reynolds number. With an increase in the Reynolds number to *Re* = 2,000, the state of the fluid near the inlet region remains unchanged. The tangential Reynolds number is larger than the axial Reynolds number indicating the occurrence of vortex breakdown. Towards tube outlet, the tangential Reynolds number approaches, but it does not intersect, the axial Reynolds number. This means that near the tube outlet, the flow state approaches the onset of vortex breakdown as indicated by the Rossby number in figure 3. For the highest Reynolds number (*Re* = 5,000), there is obviously the widest gap between the tangential Reynolds number and the axial Reynolds number near the tangential inlets. Vortex breakdown in this case takes place over the entire tube length, because the tangential and axial Reynolds number do not intersect.

A connection between the Rossby number (*Ro*), equation (5), indicating vortex breakdown and the global TSC function (Π), equation (9), characterising processes due to the velocity field redistribution on the swirl flow as shown in Figure 3, where the black straight line indicates the critical value of the Rossby number of 0.65. All Rossby numbers larger than the critical Rossby number indicate no vortex breakdown. Figure 3 supports the results from figure 2, so vortex breakdown occurs over the entire tube length for *Re* = 5,000. For *Re* = 2,000, there is a difference between numerics and experiment. Analysis of the experiments show the occurrence of vortex breakdown over the entire tube length, but analysis of numerics predicts no vortex breakdown in the region near the tube outlet. This disagreement may be assigned to a slight inaccuracy of the numerical prediction of the axial velocity and to the difference in values of the global TSC function near the tangential inlets. In case of *Re* = 1,000, vortex breakdown is predicted in the tube region where the flow is swirl dominant. Near the tube outlet, no vortex breakdown is assumed.

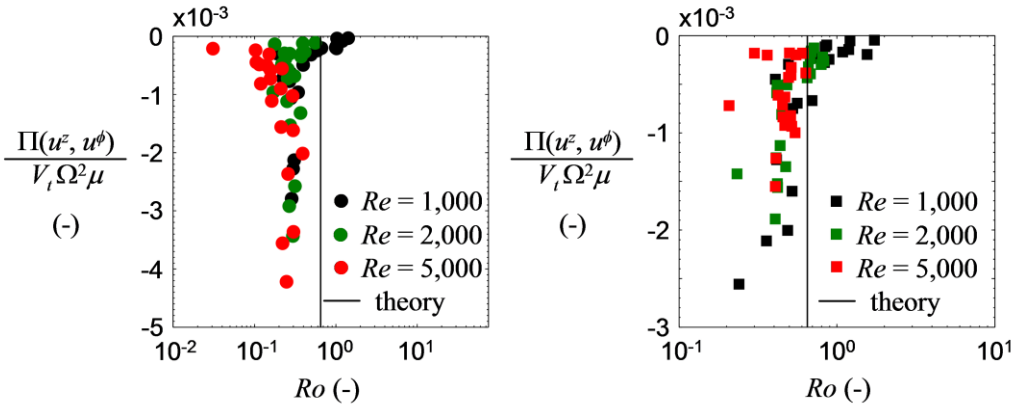


**Figure 3.** Values of the global TSC function against Rossby number. Bullets and squares represent experiment and numerics, respectively.

Values of the global TSC function, computed for the axial and tangential velocity, decrease towards tube outlet. Thus, for all investigated Reynolds numbers, as the fluid flows towards tube outlet, the global TSC function approach less negative values and the flow is stabilised from point of view of thermodynamics. The local Rossby number increases in region near the tube outlets for $Re$ = 1,000, where the flow is axial dominant. In the case of $Re$ = 2,000, the local Rossby number also increases in the region near the tube outlet, but this increase is not so significant as in the case of $Re$ = 1,000. This is due to the fact that in this case the flow is neither axial nor swirl dominant, so that the Rossby numbers are very close to the limiting value in this region. For swirl dominated flow, i.e. in case of $Re$ = 5,000, the local Rossby number decreases in the region near tube outlet. This decrease corresponds to a decrease of the swirl strength as the fluid moves towards tube outlet.

## 4. Summary and conclusions

An analysis of a swirl flow in a tube has been shown. The flow shows velocity redistribution. A prediction of vortex breakdown together with thermodynamic aspects of the flow, were presented.

We provided a description of experimental and numerical work carried out to obtain the velocity field of the swirl flow in the tube at several positions that are necessary for an analysis of vortex breakdown. Three Reynolds number were investigated, i.e. $Re$ = 1,000, 2,000 and 5,000, to cover laminar, intermediate and turbulent flow regimes. To predict vortex breakdown, the methodology based on the Rossby number was employed. Moreover, vortex breakdown and its prediction were investigated via the change of the axial and tangential Reynolds numbers showing that vortex breakdown may be expected when the flow is swirl dominated, i.e. $Re_\phi > Re_z$, and when an axial backflow occurs. This condition is fully satisfied only in case of the investigated Reynolds number $Re$ = 5,000. In the other two cases, vortex breakdown covered only part of the tube length ($Re$ = 1,000) or almost the whole tube length except a region near the tube outlet ($Re$ = 2,000).

Furthermore, a thermodynamic perspective, i.e. the TSC function introduced by equation (9), of the swirl flow together with the occurrence of vortex breakdown was presented. This analysis confirmed outcomes from the analysis based on the Rossby number and the axial and tangential Reynolds numbers. Moreover, the TSC function provided information on the redistribution of momentum and its impact on the dissipation processes taking place in the flow. It was shown that towards tube outlet, the swirl flow became more stable indicating a more pronounced potential character of the flow. This behaviour was observed for all three investigated cases.

So, the swirl flow can be analysed by the prediction of vortex breakdown based on the Rossby number. Furthermore, a decrease of the swirl strength towards tube outlet is able to be figured out by the analysis of a change in trend of the axial and tangential Reynolds number. Moreover, decrease of

the swirl strength results in a redistribution of momentum accompanied by dissipation processes in the flow field. This redistribution causes a stabilisation of the flow from thermodynamic point of view.

**Acknowledgments**
The result was developed within the CENTEM project, reg. no. CZ.1.05/2.1.00/03.0088, co - funded by the ERDF as part of the Ministry of Education, Youth and Sports OP RDI programme, and, in the follow - up sustainability stage, supported through the CENTEM PLUS (LO1402) by financial means from the Ministry of Education, Youth and Sports under the National Sustainability Programme I. The authors, B. Weigand and C. Biegger, would like to acknowledge financial support by the Deutsche Forschungsgemeinschaft (DFG) for Project WE2549/38-1.

**References**
[1] Ranque G J 1933 *J. Phys. Radium* **4** (7) 112
[2] Hilsch R 1947 *Rev. Sci. Instrum.* **18** (2) 108
[3] Pfitzer H and Beer H 1992 *Int. J. Heat Mass. Transf.* **35** (3) 623
[4] Pfitzer H 1992 Konvektiver Wärmetransport im axial durchströmten Ringspalt zwischen rotierenden Hohlwehlen, PhD thesis (Technische Hochschule Darmstadt: Institut für Technische Thermodynamik) 132
[5] Rothe T 1994 Der Einfluß der Rotation af die Strömung und den Wärmetransport im turbulent durchströmten Ringspalt zwischen zwei rotierenden Wellen, PhD thesis (Technische Hochschule Darmstadt: Institut für Technische Thermodynamik) 156
[6] Reich G, Weigand B and Beer H 1989 *Int. J. Heat Mass. Transf.* **32** (3) 563
[7] Weigand B and Beer H 1992 *Int. J. Heat Mass. Transf.* **35** (7) 1803
[8] Weigand B and Beer H 1994 *Appl. Sci. Res.* **52** (2) 115
[9] Hartnett J P and Eckert E R G 1957 *J. Heat Transfer* **79** 751
[10] Ligrani P M, Hedlund C R, Babinchak B T, Thambu R, Moon H - K and Glezer B 1998 *Exp. Fluids* **24** (3) 254
[11] Glezer B, Moon H - K, Kerrebrock J, Bons J and Guenette G 1998 Heat Transfer; Electric Power; Industrial and Cogeneration (Stockholm) **4** (New York: *American Society of Mechanical Engineers (ASME)*)
[12] Sarpkaya T 1971 *AIAA J.* **9** (9) 1792
[13] Lucca - Negro O and O'Doherty T 2001 *Prog. Energy Combust. Sci.* **27** (4) 431
[14] Escudier M 1988 *Prog. Aerosp. Sci.* **25** (2) 189
[15] Hall M G 1972 *Annu. Rev. Fluid Mech.* **4** 195
[16] Spall R E, Gatski T B and Grosch C E 1987 *Phys. Fluids* **30** (11) 3434
[17] Squire H B 1960 Analysis of the "vortex breakdown" phenomenon part 1 *Tech. rep.* (102) London: Imperial College London, Department of Aeronautics
[18] Benjamin T B 1965 *J. Basic Eng.* **87** (2) 518
[19] *ANSYS CFX - Solver Theory Guide* Release 12.0 2009 Canonsburg: ANSYS 261
[20] Alekseenko S V, Kuibin P A and Okulov V L 2007 Theory of Concentrated Vortices Heidelberg: *Springer* 494
[21] Moisy F 2012 Ezyfit: A free curve fitting toolbox for Matlab v 2.41 http://www.fast.u-psud.fr/ezyfit/
[22] Marsik F 1989 *Acta Phys. Hung.* **66** (1) 195
[23] Marsik F, Kobiela B, Novotny P and Weigand B 2010 *Proc. 21st Int. Symp. on Transport Phenomena (Kaohsiung)* (Kaohsiung: National Kaohsiung University of Applied Sciences)